J. Fluid Mech. (1981), *vol.* 108, *pp.* 423–442
Printed in Great Britain

The effects of surface topography on momentum and mass transfer in a turbulent boundary layer

By R. A. DAWKINS† AND D. R. DAVIES
Department of Mathematics, University of Exeter, U.K.

(Received 19 March 1980 and in revised form 10 November 1980)

An approximate, conveniently applied theory with corresponding experimental data is presented concerning the changes in momentum and mass transfer produced by a ridge of small slopes in a flat-surface quasi-stationary turbulent boundary layer. A first-order mean velocity perturbation solution is found to be in good agreement with measured velocities on the up-slope side of a two-dimensional ridge, of length 20 cm and height 1 cm, fixed on the floor of the working section of an open-circuit wind tunnel. A vapour-transfer eddy-diffusivity distribution is then calculated for the inner boundary-layer region and solutions of the consequent vapour-transfer equation give the variation of rate of evaporation from surfaces of varying lengths placed at different positions on the up-slope region of the ridge. Corresponding measurements are found to be in good agreement with the theoretical calculations, and show that, even over small slopes (of 1 in 10), the evaporation rate varied with position by 25% from maximum to minimum. This method of calculation is extended to examine the effect of surface curvature on diffusion of gas from an upstream line source in a turbulent boundary layer over the ridge; experimental and theoretical concentration profiles compare extremely well over the leading slope.

1. Introduction

Solutions have recently been constructed, e.g. Jackson & Hunt (1975), to give the mean velocity distribution in the flow of a turbulent boundary layer over a low hill. They were designed to apply primarily in a meteorological context. They are not specifically concerned with, for example, the problem of evaporation in wind-tunnel conditions, in which the transfer of vapour depends crucially on the structure of turbulence in an inner layer very close to the surface. Consequently an alternative mathematically convenient form of approximate analysis is developed which can be used to construct spatial distributions of eddy viscosity and vapour eddy diffusivity.

The essential controlling parameter is the downstream pressure gradient induced by the curvature of the boundary surface. It is difficult to evaluate in a turbulent boundary layer for a given shape of surface. However, it has been rigorously shown by Sykes (1980) that the leading-order velocity perturbations are associated with the appropriate inviscid, irrotational potential-flow solutions and consequently the large leading-order pressure perturbations are given by these solutions. This is the basic assumption made in this paper, and the consequences are tested in wind-tunnel

† Present address: British Aerospace, Kingston-upon-Thames, U.K.

conditions. A mean (logarithmic) velocity profile, changing very slowly with downstream distance, is perturbed by a two-dimensional ridge of small slopes fixed on the floor of the working section of a wind tunnel. The particular curved-ridge surface studied is then identified with a streamline of an equivalent inviscid potential flow past a circular cylinder, noting that it can be generalized by considering other cylindrical surfaces; Bernoulli's theorem then gives an expression for the downstream variation of pressure gradient, which is inserted into the equation of mean turbulent flow. By using the premise that the structure of turbulence near the ridge surface is similar to that in classical flat-plate flow and that the downstream pressure gradient is an order of magnitude greater than the variation of turbulent shearing stress induced by the small slope, the first-order perturbation induced by the curvature in the logarithmic mean velocity profile can be evaluated. These results are then tested by comparing computed mean velocity profiles at various positions on the ridge with measured values. The measured profiles demonstrate the complex effect of curvature and are valuable in themselves, as measurements of this type have not previously been obtained in detail (as indicated by Jackson & Hunt 1975). They were found to be in excellent agreement with the theoretical profiles except for a region very close to the surface on the lee side of the brow of the ridge.

The distribution of eddy viscosity was then evaluated for the limited downstream ridge lengths considered. The eddy-diffusivity distribution in the inner layer adjacent to these limited areas of ridge surface follows by applying Reynolds analogy, and a convenient method of calculating evaporation (Davies & Bourne 1956) can be used. This is valid for cases in which the thickness of the momentum boundary layer varies significantly in the downstream direction, and contains a vapour boundary layer whose thickness also varies in this direction. The method of calculation is then verified by carrying out a series of experiments employing the gravimetric method of measuring evaporation from surfaces of aniline of different lengths placed on different locations on the upslope ridge surface, and the effect of curvature on evaporation estimated.

Finally, a method is described of predicting concentration profiles over a ridge when a line source of gas is placed upstream, in wind-tunnel conditions: this process does not appear to have been previously studied in detail. The two-dimensionality of the problem restricts its applicability, but the results indicate the considerable changes in gas concentration caused by a curved surface on a turbulent boundary layer. The eddy-diffusivity distribution in the inner layer, used to calculate evaporation, does not give good results for concentration profiles, and an expression for eddy diffusivity, applied by Davies & Bourne (1956) over the main thickness of the boundary layer, is modified by assuming an approximate similarity in shape of the velocity profiles over the limited range of the leading slope of the ridge. A solution of the two-dimensional equation is obtained, and experiments on gas concentration distributions over a ridge surface in a wind tunnel are used to test the method of calculation.

2. Distribution of velocity profiles over a ridge surface

(*a*) *Theoretical analysis*

In order to derive a suitable expression for the pressure distribution created by the motion of air over the ridge, two-dimensional inviscid incompressible flow theory is

used. An application of this to the flow around a circular cylinder, radius a, inserted into a uniform stream U_0 moving along a negative X axis, leads to a stream function in the form

$$\psi = U_0\left(Y - \frac{a^2 Y}{X^2+Y^2}\right), \tag{1}$$

and a pressure distribution, given by

$$p(X, Y) = \tfrac{1}{2}\rho U_0^2[2a^2(X^2-Y^2)-a^4]/(X^2+Y^2)^2, \tag{2}$$

where ρ denotes air density and (X, Y) refer to positions parallel to and perpendicular to U_0, relative to the centre of the cylinder. An expression for the pressure variation along a given streamline, $\psi = \psi_0$ (constant), is next required and substituted into the classical (logarithmic) mean velocity profile of a flat-plate turbulent boundary layer, with the assumption that $p(X)$ is a function of downstream distance only, in the boundary layer. In this way an estimate is made of the modification created in the flat-plate profile by a small downstream curvature. Substitution of (1) into (2) leads, however, to a complex expression for $p(X)$ and a streamline form for a curved boundary surface which would be difficult to cut for wind-tunnel experimentation.

As an initial test of the complex effect of surface curvature, the limiting case is considered of small slope expressed by taking the parameter (aU_0/ψ_0) to be small and expanding in powers of this parameter. This leads to the downstream pressure distribution

$$\begin{aligned} p(X)/\tfrac{1}{2}\rho U_0^2 = {} & \{2(aU_0/\psi_0)^2[((X/L)^2-1)((X/L)^2+1)^2 - 2(aU_0/\psi_0)^2((X/L)^2+1) \\ & - (aU_0/\psi_0)^4] - (aU_0/\psi_0)^4((X/L)^2+1)^2\}(1+(X/L)^2)^2 \\ & \times[(1+(X/L)^2)^3 + 2(aU_0/\psi_0)^2(1+(X/L)^2) + (aU_0/\psi_0)^4]^{-2} \end{aligned} \tag{3}$$

by neglecting higher-order terms in (aU_0/ψ_0); $\psi_0/U_0 = L$ is a convenient length scale. The associated shape of surface

$$y/L = 1 + (aU_0/\psi_0)^2[1+(X/L)^2]^{-1} \tag{4}$$

is a convenient section for wind-tunnel preparation.

We now consider a fully developed turbulent boundary layer on the flat lower surface of a wind tunnel, sufficiently far downstream of the virtual origin of the turbulent boundary layer to be considered independent of downstream distance over the extent of the ridge. From wind-tunnel experiments in this region, we find it possible to represent very closely a simplification to the logarithmic profile in the form

$$\bar{u} = Ay^p, \tag{5}$$

y being measured along a normal from the tunnel surface. Values of A and p and the experimental profiles are shown in figure 1 using the experimental technique described in § 2(*b*).

A ridge of small slope is now inserted and the consequent change in velocity distribution found when the pressure distribution (3) is inserted into the flat-plate boundary-layer profile, represented by (5). The two-dimensional equation of mean motion to be solved is then

$$u\frac{\partial u}{\partial x} + v\frac{\partial u}{\partial y} = -\frac{1}{\rho}\frac{\partial p}{\partial x} + \frac{\partial}{\partial y}\left(\epsilon\frac{\partial u}{\partial y}\right), \tag{6}$$

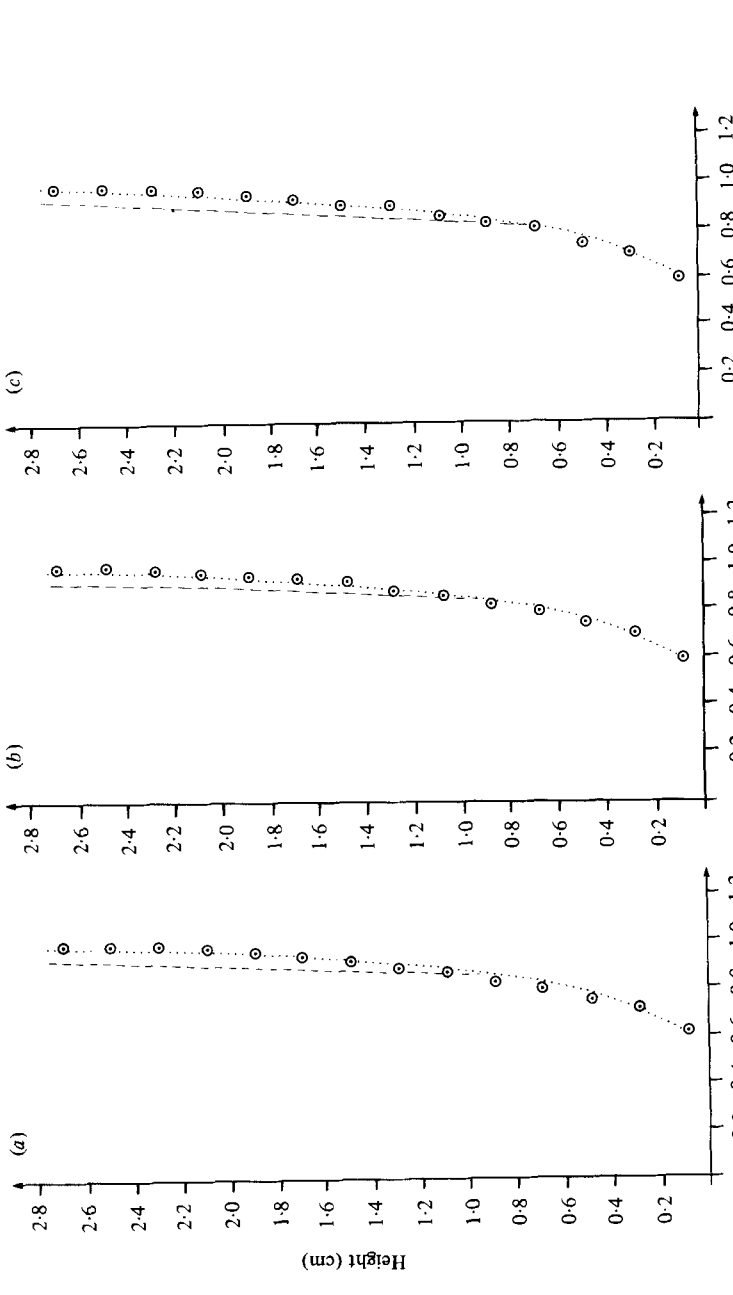

FIGURE 1. Mean velocity profiles over a flat surface: ⊙⊙⊙⊙, experimental points: ——, $u/u_\tau = 5{\cdot}5 + 2{\cdot}5 \ln (u_\tau y/\nu)$. (*a*) $u_0 = 1540$ cm/s, $u_\tau = 62$ cm/s; · · ·, $u = 1305y^{0{\cdot}15}$. (*b*) $u_0 = 1870$ cm/s, $u_\tau = 74$ cm/s; · · ·, $u = 1585y^{0{\cdot}15}$. (*c*) $u_0 = 2150$ cm/s, $u_\tau = 83$ cm/s; · · ·, $u = 1820y^{0{\cdot}15}$.

x being downstream distance from virtual origin of the boundary layer, and u and v are mean velocities, ϵ is the eddy viscosity, and Reynolds stress τ is taken to be related to ϵ by the gradient relationship $\tau/\rho = \epsilon\,\partial u/\partial y$.

We now assume that the dominant term on the right-hand side of (6) is $\partial p/\partial x$; this is consistent with the result obtained by the rigorous analysis of Sykes (1980) and our basic premise that the structure of turbulence is similar in flat-plate and small-ridge flow. It is also justified by the very close agreement found between experimental and theoretical profiles. We then write $u = \bar{u} + \hat{u}$, $v = \hat{v}$, where $\hat{u}$ and $\hat{v}$ are the small modifications produced by the presence of the ridge. Neglecting second-order small terms, equation (6) becomes

$$\bar{u}\frac{\partial \hat{u}}{\partial x} + \hat{v}\frac{\partial \bar{u}}{\partial y} = -\frac{1}{\rho}\frac{\partial p}{\partial x}, \tag{7}$$

which after substitution of (5) and use of the continuity equation leads to the solution

$$\hat{u} = \frac{-(1-p)}{(1-2p)\,A}\,y^{-p}\,[p(x)/\rho - p(x_1)/\rho] + pc_0 y^{p-1}x + \hat{U}_0, \tag{8}$$

where $\hat{U}_0$ is the perturbed profile at $x = x_1$, $p(x_1)$ is the dynamic pressure at any specific value of $x = x_1$ due to the ridge and c_0 is an arbitrary constant. To be consistent with two-dimensional potential-flow theory, we assume $\hat{u}$ is symmetric about the highest point of the ridge and so $c_0 = 0$. As $y \to 0$ a different form of analysis is required and is found by matching $\hat{u}$ values to the classical empirical logarithmic formulae for mean velocity in a turbulent boundary layer near a flat surface.

(*b*) *Experimental method and results*

The wind tunnel used is housed in a very large laboratory with a high ceiling in the Applied Science Building at Exeter University. It is a traditional open-circuit, low-speed system, designed by Dr F. M. Burrows (University College of North Wales, Bangor) and is well tested by Applied Science staff at Exeter: its overall length is 10·5 m, the working section being 1·5 m long, 0·9 m wide, and 0·5 m high. The floor of the working section is in four removable sections. The maximum possible speed of air in the working section is approximately 40 m s^{-1} but the maximum speed used was 20 m s^{-1} to avoid any effect of wall vibration on the turbulent boundary overlying the flat working-section surface; mean velocity profiles were measured for flow speeds of 1540, 1870, 2150 cm s^{-1}. These velocity measurements were made along the centre-line of the section using a standard Pitot-tube system; atmospheric pressure and temperature were also measured in order to correlate the results. Vertical distances could be measured at intervals of 0·01 mm, but measurements at intervals of 0·5 mm were sufficient to define the profiles; however, due to the magnitude of the outer diameter of the available Pitot tube the nearest reading to the surface was at 0·8 mm.

Measurements of velocity profiles were first taken over two of the floor sections to check (*a*) that the virtual origin of the turbulent boundary layer (obtained by plotting the heights of points at which $u/U_0 = 0{\cdot}99$) was well upstream of the particular floor section used in the experiments, and (*b*) that (before insertion of a ridge) the thickness of the layer did not change appreciably with downstream distance over the range, 20 cm, of the ridge position. A rectangular inset of 0·6 cm deep, 30 cm wide, and 20 cm long was then cut into this section. The two-dimensional ridge was made out of Perspex 1·6 cm high, 30 cm wide, and 20 cm long, and fitted into the inset.

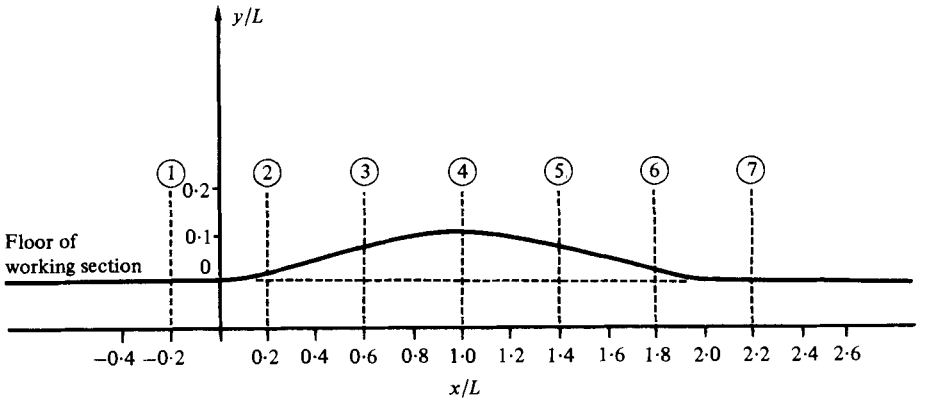

FIGURE 2. ——, cross-section of ridge surface; ○, sampling positions 1 to 7.

The ridge was manufactured by a numerically controlled milling and drilling machine, programmable with the aid of a punched paper tape; full details of this and related processes are given by R. A. Dawkins (1979). Suitable holes were drilled along the centre-line of the ridge at positions shown in figure 2, and brass tubes were fixed underneath these, along which the Pitot tube could be traversed vertically; before using a particular sampling position the other holes were suitably covered.

The surface of the ridge was cut to the shape shown in figure 2, and given by

$$y/10 = 0{\cdot}2/[(\bar{x}/10)^2 - 2(\bar{x}/10) + 2], \tag{9}$$

obtained from equation (4) by taking $L = 10$ cm, $(aU_0/\psi_0)^2 = 0{\cdot}2$, and $\bar{x}$ is now the downstream distance from the leading edge of the ridge. The effect of neglecting terms of order $(aU_0/\psi_0)^4$ is found to be small for these numerical values of L and (aU_0/ψ_0); the error in the expression for $p(X)$, equation (3), is found to be only of order 3 %, with a similar small error in (9). It is not, of course, possible in practice to arrange a ridge of infinite extent on the floor of the working section; consequently the length of the ridge actually tested was terminated at $\bar{x} = 0$ and $2L$ in the new co-ordinate, and the measured velocity profile at position 1 (figure 2) taken as an initial upstream condition.

Substitution of $(aU_0/\psi_0)^2 = 0{\cdot}2$ in equation (3) gives the variation of $p(x/L)$ with x/L; it is shown in figure 3. The theoretical modification to mean downstream velocity (equation (8)) is of the form

$$\hat{u} = -\frac{(1-p)\,p(x/L)\,y^{-p}}{A(1-2p)\rho} + g(y), \tag{10}$$

where $g(y)$ is the form $c_1 y^{-p}$ which would be zero if the whole infinite ridge was inserted into the flow. However, since the ridge is terminated by practical wind-tunnel conditions, it is necessary to determine a value for c_1 from a measured profile at one specific downstream position: this was taken at the leading edge of the ridge, at position 1 (marked in figure 2), for each value of U_0 used. Taking this as a necessary initial condition due to practical limitations, it is, of course, nevertheless a good test of theory to compare measured and calculated $(\bar{u} + \hat{u})$ values at the downstream sampling points numbered 2–7. The values of the constant c_1 were found to be -128, -155, -179 for $U_0 = 1540$, 1870, 2150 respectively (all in units of cm s^{-1}).

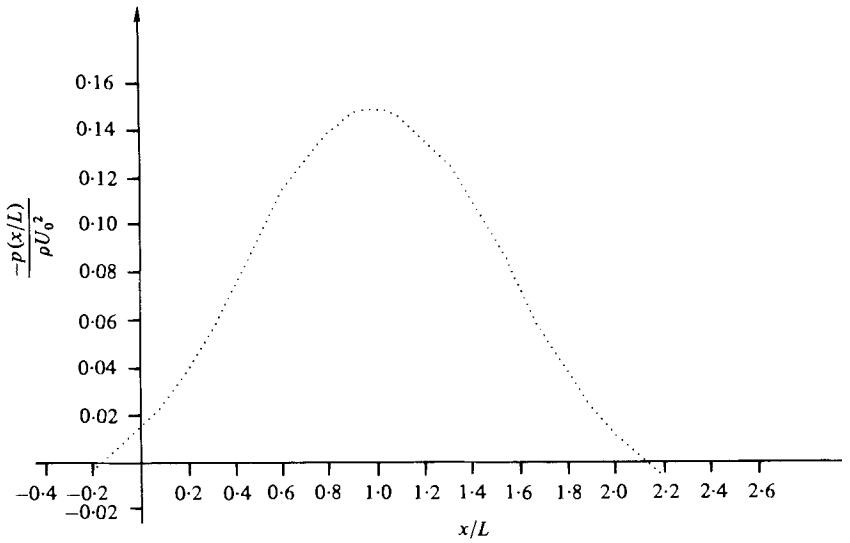

FIGURE 3. Calculated pressure distribution over the ridge (given by equation 9).

Figures 4(*a*)–4(*g*) give $u = \bar{u} + \hat{u}$ at positions 1–7, and show that the calculated theoretical profiles are in good agreement with measured ones, except in the region between 1 and 4 mm for positions 5 and 6 on the lee side of the ridge. In this region the pressure gradient term is reduced; the discrepancy between the results of approximate theory and experiment suggests that a higher-order theory is needed, involving a contribution from Reynolds stresses. The velocity profile at position 4 (figure 4*d*) shows clearly the sharp increase in velocity (about 30 %) due to the effect of curvature on the pressure gradient distribution, and suggests that the local evaporation from a wet surface (or heat from a heated surface) and consequent diffusion in the region of flow above, is also sensitive to curvature. These experimental profiles may also fill a need (as indicated in § 1) to have available good velocity profile data for flow over a ridge in wind-tunnel conditions.

It was not possible to measure velocity profiles in a region of less than 1 mm from the surface but, as this is the region which strongly influences vapour (or heat) transfer from the surface, it is necessary to make an estimate of the mean velocity distribution in this inner layer. The theoretical velocity values $(\bar{u} + \hat{u})$ close to the surface (these fit observed values closely) are matched to those given by the classical flat-plate empirical equation (e.g. see Howarth 1953, p. 824),

$$u/U_\tau = 5{\cdot}5 + 2{\cdot}5 \ln y_\tau \quad \text{for} \quad y_\tau > 30, \tag{11}$$

where $y_\tau = U_\tau y/\nu$, ν is the kinematic viscosity and U_τ is the 'friction velocity', whose values are thus determined. The structure of turbulence very near the slightly curved surface is then assumed to be similar to that near a flat-plate surface. Figures 5(*a*), (*b*) show the approximate fit for stations 1–4 at $U_0 = 2150$ cm s^{-1}. The resulting calculated downstream variation of U_τ on the upslope side of the ridge is shown in figure 6(*a*). This is a linear relationship of the form $U_\tau = \alpha(\bar{x} + \beta)$, where $\alpha = 3{\cdot}10$ and $\beta = 23{\cdot}97$ cm at $U_0 = 2150$ cm s^{-1}, and $\bar{x}$ is in cm measured from the leading edge of the ridge.

These values can now be used to construct a convenient approximate mathematical

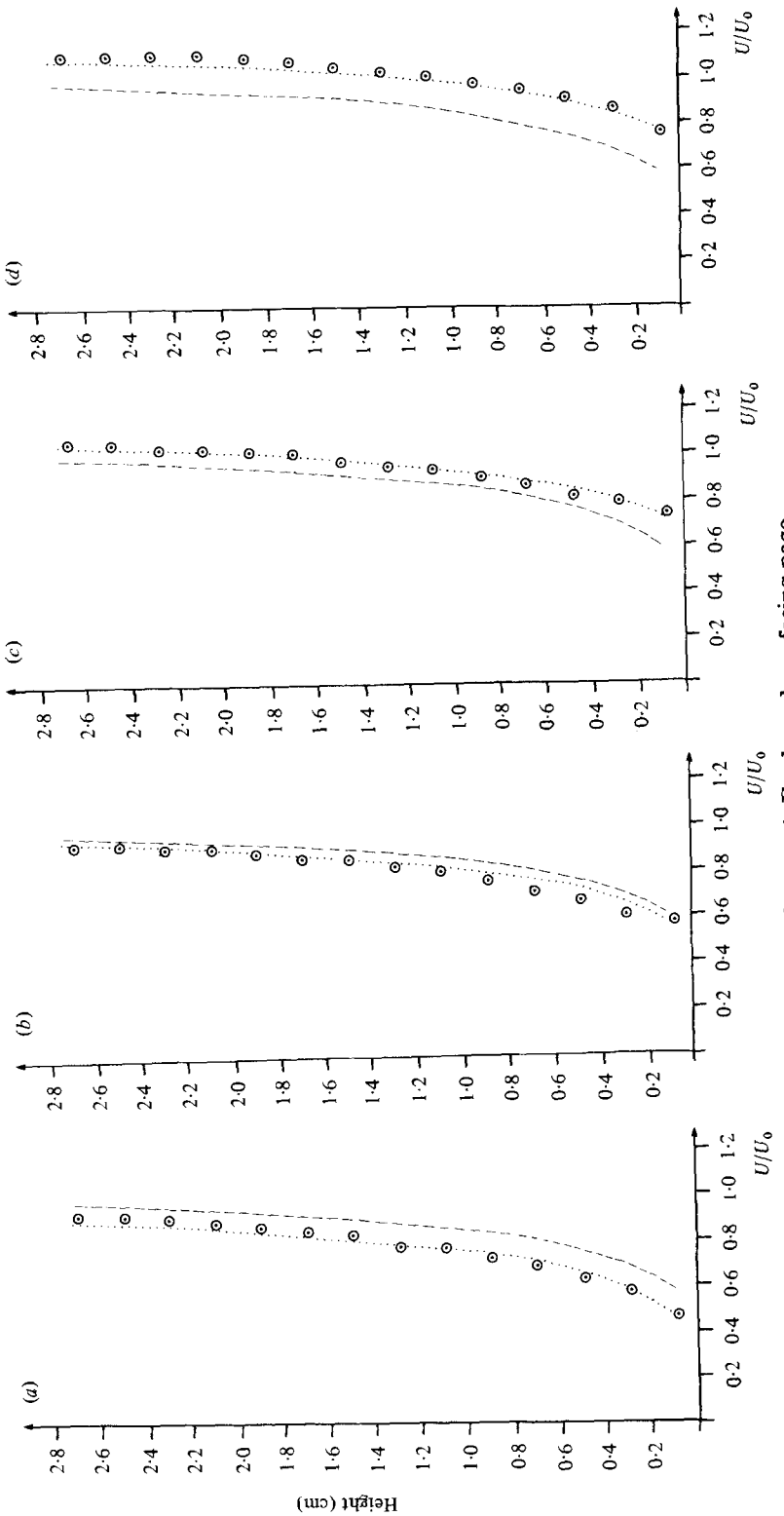

FIGURE 4. For legend see facing page.

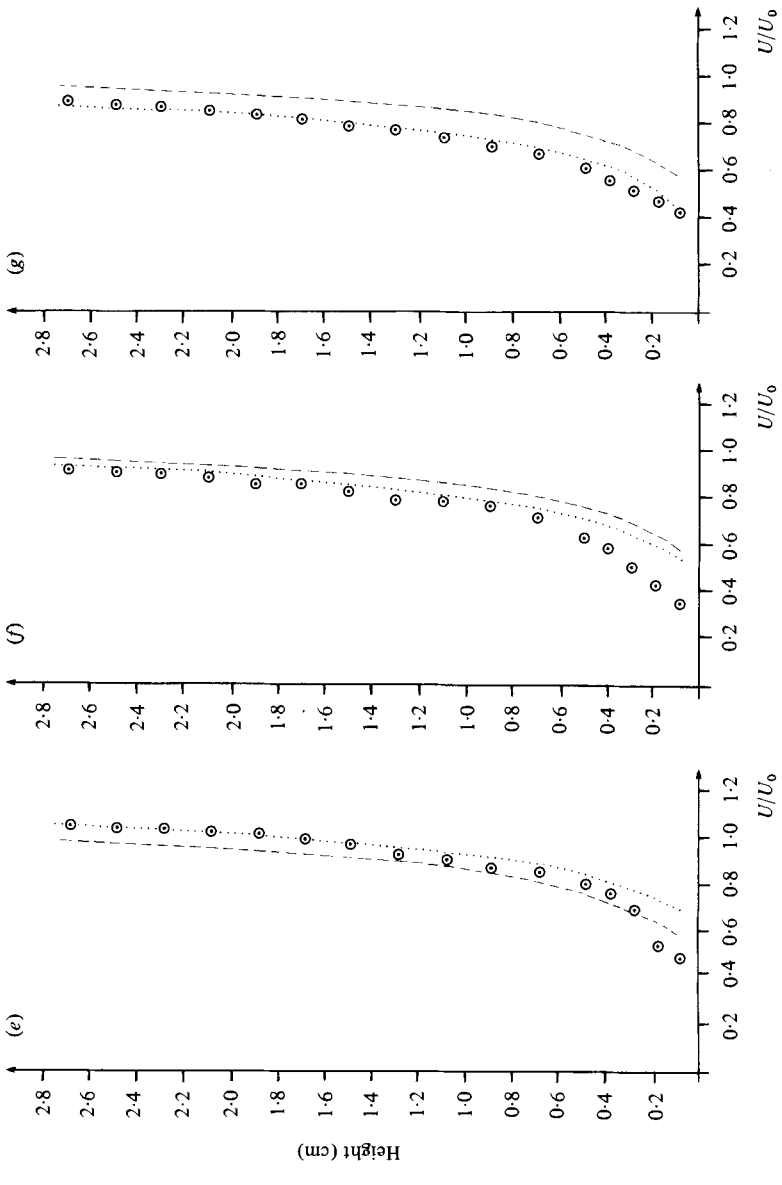

FIGURE 4. Mean velocity profiles at various sampling positions (defined in figure 2) over the ridge: $u_0 = 2150$ cm/s; ---, $\bar{u} = 1820y^{0.15}$; ⊙⊙⊙, experimental points; · · ·, calculated $\bar{u}+\hat{u}$; (*a*) position 1, (*b*) position 2, (*c*) position 3, (*d*) position 4, (*e*) position 5, (*f*) position 6, (*g*) position 7.

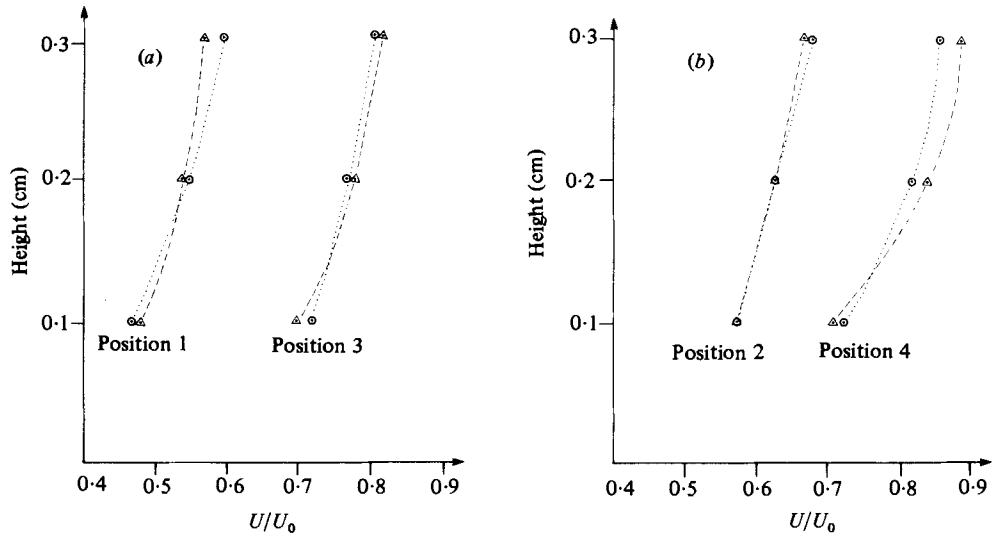

FIGURE 5. Approximations to mean velocity profiles near the ridge surface: $u_0 = 2150$ cm/s: ---△---, $u/u_\tau = 5{\cdot}5 + 2{\cdot}5 \ln(u_\tau y/\nu)$; ··· ⊙ ···, theoretical u/u_0. (*a*) position 1, $u_\tau = 69$ cm/s and position 3, $u_\tau = 95$ cm/s. (*b*) position 2, $u_\tau = 79$ cm/s and position 4, $u_\tau = 102$ cm/s.

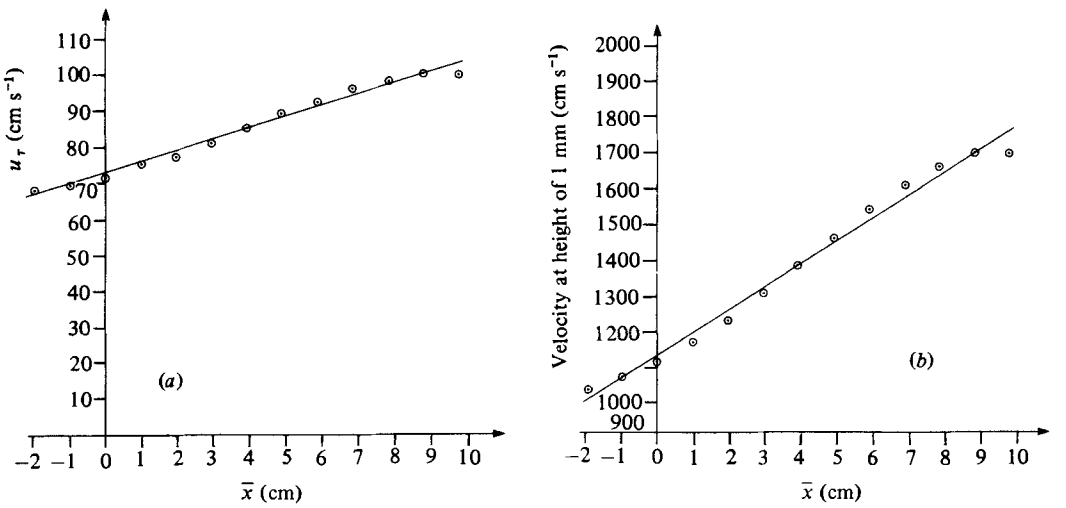

FIGURE 6. (*a*) Estimated downstream ($\bar{x}$) variation of friction velocity, u_τ, over the ridge. (*b*) Estimated downstream variation of velocity at height of 1 mm over the ridge surface. $\bar{x}$ is measured from leading edge of ridge.

description of the mean flow distribution in the region very close to the surface, which controls evaporation. The lowest height at which velocity can be measured by the available apparatus is 0·1 cm. The variation of this velocity, $u_{0\cdot1}$, is shown in figure 6(*b*): it is found by fitting a line of regression to this data. A good representation is found in the form $u_{0\cdot1} = b\zeta^r$, where $\zeta = \bar{x} + \beta$. For $U_0 = 2150$ cm s^{-1}, $b = 10{\cdot}61$, $r = 1{\cdot}35$: for $U_0 = 1870$ cm s^{-1}, $b = 13{\cdot}39$, $r = 1{\cdot}33$: for $U_0 = 2150$ cm s^{-1}, $b = 17{\cdot}41$, $r = 1{\cdot}31$: ζ in cm. In the direction normal to the surface a power-law variation is used, since this has been seen to lead to a good representation from 2 to 30 mm from the surface and

it is also required to apply available evaporation theory in a developing turbulent boundary layer. So the form

$$u = b\zeta^r(y/0{\cdot}1)^q \tag{12}$$

is used as a convenient approximate description of the mean flow field in the region over the leading slope in the inner layer, close to the ridge surface. The value of $q = 0{\cdot}15$ was found to give a good fit to the logarithmic empirical form and also to the measured data for heights up to 30 mm.

3. Spatial distribution of rate of evaporation along the leading slope of a ridge surface

(*a*) *Theoretical analysis*

The problem of evaporation from a flat saturated liquid surface into a fully turbulent boundary layer has been initially treated theoretically by, for example, Sutton (1953) and experimentally by Pasquill (1943) and by Davies & Walters (1952). This theory assumed the velocity profile and Reynolds stress to be independent of downstream distance. Davies & Bourne (1956) modified this work to allow for variation of thickness of the momentum boundary layer with distance in which a vapour boundary layer is embedded. In the problem of flow over a ridge, along the surface of which the surface vapour concentration is supposed known, or the temperature known in the case of heat transfer, this thickness variation is quite marked and the approach of Davies & Bourne is essential.

Following their analysis the diffusion equation is

$$u\frac{\partial \chi}{\partial x} + v\frac{\partial \chi}{\partial y} = \frac{\partial}{\partial y}\left(\epsilon_D \frac{\partial \chi}{\partial y}\right), \tag{13}$$

where χ denotes the mean concentration of vapour and ϵ_D the eddy vapour diffusivity, x being measured from virtual origin of the boundary layer. Assuming that the mechanisms involved in transporting momentum are the same as those transporting vapour, we identify ϵ_D with ϵ. The downstream variation in thickness of momentum boundary layer is treated by using ψ (stream function) and x instead of y and x. As shown by Davies & Bourne, the diffusion equation is then

$$\frac{\partial \chi}{\partial x} = \frac{\partial}{\partial \psi}\left[\epsilon u \frac{\partial \chi}{\partial \psi}\right]. \tag{14}$$

The details of a solution for the curved surface then follow that given for the flat-plate case but velocity parameters derived from the curved-surface calculations are used. The velocity profile (12) was taken to represent u over the limited range of evaporating areas tested on the upwind slope of the ridge. The corresponding ϵ distribution is obtained by using $\tau/\rho = \epsilon\, \partial u/\partial y$, with $\tau = \tau_0 =$ constant, in the region from the surface up to 3 mm say (which determines evaporation or heat transfer), $= \rho U_\tau^2$, and $U_\tau = \alpha\zeta$, using x values consistent with equation (13). Hence in cm s units

$$\epsilon = \alpha^2(0{\cdot}1)^q \zeta^{2-r} y^{1-q}/bq. \tag{15}$$

Substitution of equation (12), with $u = \partial\psi/\partial y$, and integration gives

$$\psi = \frac{b}{(0{\cdot}1)^q(1+q)}\zeta^r y^{1+q}. \tag{16}$$

Consequently ϵu in terms of ψ is

$$\epsilon u = \alpha^2 q^{-1} b^{-(1+q)^{-1}} (0{\cdot}1)^{q(1+q)^{-1}} (1+q)^{(1+q)^{-1}} \zeta^{(2+2q-r)(1+q)^{-1}} \psi^{(1+q)^{-1}} \tag{17}$$

and substitution into the diffusion equation leads to

$$\frac{\partial \chi}{\partial X} = d \frac{\partial}{\partial \psi} \left[\chi^t \frac{\partial \chi}{\partial \psi} \right], \tag{18}$$

where $t = (1+q)^{-1}$, $X = \zeta^s$ with $s = (3+3q-r)(1+q)^{-1}$, and

$$d = \alpha^2 q^{-1} s^{-1} b^{-(1+q)^{-1}} (0{\cdot}1)^{q(1+q)^{-1}} (1+q)^{(1+q)^{-1}}.$$

The method of sources described in detail by Davies & Bourne (1956) for a flat surface can now be followed exactly except for the different numerical values of the parameters. They showed that, by neglecting the presence of sub-layers as a first approximation and extrapolating the velocity profile (12) right down to the actual surface, a convenient expression for evaporation from a surface of length l could be obtained, which was in good agreement with experiments over flat surfaces. Following this procedure, we find that evaporation from a length l of surface placed with leading edge at a distance of $\bar{x}$ from the leading edge of the ridge is given by

$$E = B^{(2-t)^{-1}} (2-t)^{(t+1)/(2-t)} \Gamma\{(2-t)^{-1}\} \pi^{-1} \sin \mu\pi(\chi - \chi_0) \mu^{-1} [(\zeta + l)^s - \zeta^s]^\mu, \tag{19}$$

where $B = (2-t)d$, $\mu = (2-t)^{-1}$.

The method described by Davies & Bourne of partitioning E into contributions from the sub-layers and fully turbulent regimes can be followed, but the expressions are complex, and a calculation in the ridge conditions suggested that the additional computation involved was not necessary.

(*b*) *Experimental method and results*

The evaporation experiments were based on the gravimetric method used by Pasquill, and Davies & Walters. A flat piece of Perspex was shaped to fit into the inset on the floor of the working section. Strips of Whatman No. 1 filter paper were placed on this and saturated with aniline (which has convenient vapour diffusion properties); these were of width 15 cm and lengths 3, 6 and 10 cm and can be regarded as simulating a saturated liquid surface, with a constant χ_0 value depending on temperature. The techniques of measurement as used in previous work were employed, the Perspex slab and filter paper being weighed before and after a suitable period of evaporation, an accurate electromagnetic balance being used. The method was extended to similar measurements on the up-slope region of a ridge by cutting a piece of Perspex to exactly fit the inset on the working-section floor, and shaping the upper surface to be identical with the ridge shape used previously.

Values of U_0 used were 1540, 1870, 2150 (cm s^{-1}), corresponding to downstream distances, x, of the leading edge of Perspex from the virtual origin of the turbulent boundary layer of 100, 110 and 120 cm respectively. The evaporation experiments on each specific size of evaporating area was repeated several times. The means of these, the standard deviation of each group being small, are in good agreement with theoretical results, calculated from (19) using flat-surface parameters, and serve as a check on experimental procedures. In table 2 the evaporation experimental results for various positions on the ridge are shown together with the associated theoretical results, also calculated from (19) using ridge parameters with appropriate numerical

U_0 (cm s^{-1})	l		
	3	6	10
	(*a*) Experimental results		
1540	0·018	0·035	0·052
1870	0·021	0·043	0·062
2150	0·024	0·044	0·072
	(*b*) Theoretical results		
1540	0·019	0·0345	0·054
1870	0·022	0·041	0·063
2150	0·0245	0·045	0·070

TABLE 1. Evaporation from flat surfaces in g min^{-1}, width = 15 cm and varying values of l (cm).

U_0	l	$\bar{x}$	Experimental	Theoretical
1540	3	1	0·021	0·020
		4	0·0215	0·022
		7	0·023	0·024
	6	1	0·038	0·039
		4	0·041	0·042
	10	0	0·060	0·063
1870	3	1	0·023	0·023
		4	0·025	0·025
		7	0·026	0·027
	6	1	0·045	0·045
		4	0·048	0·048
	10	0	0·070	0·072
2150	3	1	0·024	0·026
		4	0·028	0·029
		7	0·029	0·031
	6	1	0·049	0·051
		4	0·053	0·058
	10	0	0·079	0·082

TABLE 2. Evaporation from area sources on the leading slope of the ridge in g min^{-1}, width = 15 cm, varying values of l (cm), and distances $\bar{x}$ (cm) of leading edge of evaporation area from origin of ridge. Experimental and theoretical results.

values; these are seen to be also in good agreement with experimental results. They show clearly the sharp variation of evaporation with position on the ridge surface: the values for the 3 cm length area source at the highest part of the ridge are seen to be 20–25 % higher than those on the lowest part of the slope.

4. Turbulent diffusion over the leading slope of a ridge from an upstream line source

(*a*) *Theoretical analysis*

There have been several previous alternative discussions of the problem of turbulent flow and diffusion over variable-surface topography, e.g. Hunt & Mulhearn (1973),

Taylor (1977). However, as in §3, the method of analysis described by Davies & Bourne (1956) was found to be the most convenient to apply to wind-tunnel conditions. This is based on solving equation (14) using the velocity profile form (12) with an eddy-diffusivity distribution, applying over the main part of the boundary-layer thickness. Analysis of the velocity profile, equation (12), over the leading slope shows that q varies from 0·19, two centimetres upstream of the ridge, to 0·10 over the brow of the ridge, but, in order to solve the resulting equation analytically, it is necessary to assume a constant q value. The resultant velocity distribution, with $q = 0{\cdot}15$, is found to compare well with the experimental velocity profiles over the leading slope of the ridge. However, the associated eddy-diffusivity distribution based on the assumption of constant stress in the region immediately adjacent to the surface is found not to yield good agreement between theory and experimental results for the distribution of gas concentration over the main thickness of the boundary layer. Applications of mixing length did not improve agreement, and it was found necessary to express the eddy viscosity in an alternative form.

First it was noted from experimental flat-plate velocity profiles, over the limited range of downstream distance considered, that the velocity at the height of 0·1 cm is seen to be approximately 0·6 times the mainstream velocity, and we then assume that $u_{0{\cdot}1}/U_0 = 0{\cdot}6$, where U_0 is the mainstream velocity and $u_{0{\cdot}1}$ the velocity at a height of 0·1 cm above the ridge surface over the small range of downstream distance considered, replacing an actual very slow variation of $u_{0{\cdot}1}/U_0$ with x over the ridge.

Secondly, it was noted from Davies & Bourne (1956) that an expression for eddy diffusivity, based on experimental results in the flat-plate case, could be written in the form

$$\epsilon = KU_0 x^P h(\xi), \tag{20}$$

where x is the downstream distance from the virtual origin of the turbulent boundary layer, U_0 is the mainstream (flat-plate) velocity, K is a constant found from experiment, and

$$h(\xi) = 0{\cdot}00065\xi^{0{\cdot}40}, \tag{21}$$

where $\xi = y/(kx^R)$. This leads to $\epsilon = DU_0 y^m$, for a specific downstream dustance, where $m = 0{\cdot}40$, and $D = 0{\cdot}00065Kx^{(P-0{\cdot}40R)}/k^{0{\cdot}40}$. At a sufficiently distant position downstream of the start of the turbulent boundary layer, a 10 cm change in upstream or downstream distance is found to give rise to a negligible change in D, and it is assumed for mathematical convenience that the eddy viscosity depends only on vertical distance, over the limited range of x studied; a constant value of D is used corresponding to the mid-point of this range.

However, over the leading slope of the ridge the velocity at a height of 0·1 cm has been approximated in §2 by $u_{0{\cdot}1} = b\zeta^r$, and using a value of 0·15 for q in equation (12) gives a distribution of velocity profiles, over the leading slope of the ridge, which are found to be similar in shape to observed flat-plate velocity profiles. Therefore, it is assumed that the flow at the height of 0·1 cm over the leading slope of the ridge behaves as if it is in a turbulent boundary layer over a flat plate with a varying mainstream velocity. With $U_0 = b\zeta^r/0{\cdot}6$, the associated expression for eddy viscosity, (7), becomes

$$\epsilon = Db\zeta^r y^m/0{\cdot}6. \tag{22}$$

Using the analysis described in § 3 with appropriate x values, a solution of equation (14), with expression (12) and (20) substituted for u and ϵ respectively, gives an expression for the concentration downstream of a line source over the leading slope of a ridge in a wind tunnel in the form

$$\chi - \chi_0 = A\eta^{-(2-\tau)^{-1}} \exp\{-\omega^{(2-\tau)} B^{-1} (2-\tau)^{-1}\}, \tag{23}$$

where χ_0 is the mean concentration of diffusing matter upstream of the line source. The values of the parameters are given by

$$A = Q[B^{(2-\tau)^{-1}} (2-\tau)^{(\tau-1)/(2-\tau)} \Gamma\{(2-\tau)^{-1}\}]^{-1},$$

$$\tau = \frac{m+q}{1+q},$$

$$B = \frac{D(1+q)^{(m+q)/(1+q)} (0{\cdot}1)^{q(m-1)/(1+q)} b^{(2+q)/(1+q)} (2+q-m)}{0{\cdot}6((2+q-m)r+1+q)},$$

$$\eta = \zeta^s - \zeta_0^s = (\bar{x}+\beta)^s - (\bar{x}_0+\beta)^s,$$

$$\omega = \psi\eta^{-(2-\tau)^{-1}}, \quad \psi = \frac{b\zeta^r y^{(1+q)}}{(0{\cdot}1)^q (1+q)}, \quad s = \frac{r(2+q-m)+1+q}{(1+q)}$$

and Q is the rate at which matter is being emitted from the line source per unit width: $\bar{x}$ refers to downstream distance from origin of the ridge, $\bar{x}_0$ and ζ_0 corresponding to the line source position. Equation (23) is then used to determine the concentration profiles at specific stations over the leading slope of the ridge.

(*b*) *Experimental method and results*

The apparatus described in § 2 for the momentum transfer case was adapted to obtain the experimental data. A slit 0·02 cm long and 27·5 cm wide was made out of brass and inserted into the floor section upstream of the start of the ridge, so that the leading edge of the ridge was 1·6 cm downstream. The uniformity of the slit was ensured by putting fixing screws across its width and a toolmaker's microscope was used to set the narrow gap. A large hollow metal construction was welded under the slit and by way of a manifold the cavity formed was connected to a nitrous oxide source. The size of the cavity under the slit is important, since it is necessary to ensure that the nitrous oxide escaped uniformly across the width of the slit. Before any concentration profiles are measured, experiments are performed to ascertain whether the gas emitted from the slit makes any measurable difference to the existing turbulent boundary layer. For the rates of flow of gas at which the experiments are to be performed, the apparatus used for measuring pressure differences in the boundary layer failed to detect any difference, for both the flat-plate and ridge cases.

The Pitot tube was placed in position, as in the momentum transfer experiments, and then connected to a gas analyser and electric pump. Hence mixtures of air and nitrous oxide are drawn into the gas analyser via the mouth of the Pitot tube. The concentration thus obtained is taken as the average over the mouth of the Pitot tube. A Grubb–Parsons gas analyser is used; for further details of experimental methods see R. A. Dawkins (1979).

Firstly a flat plate is placed in the downstream position of the ridge and measurements made at various downstream stations; calculations based on the analysis by Davies & Bourne (1956) are then compared with the experimental data. It can be seen from figure 7 that the theory agrees extremely well with the experiments. The

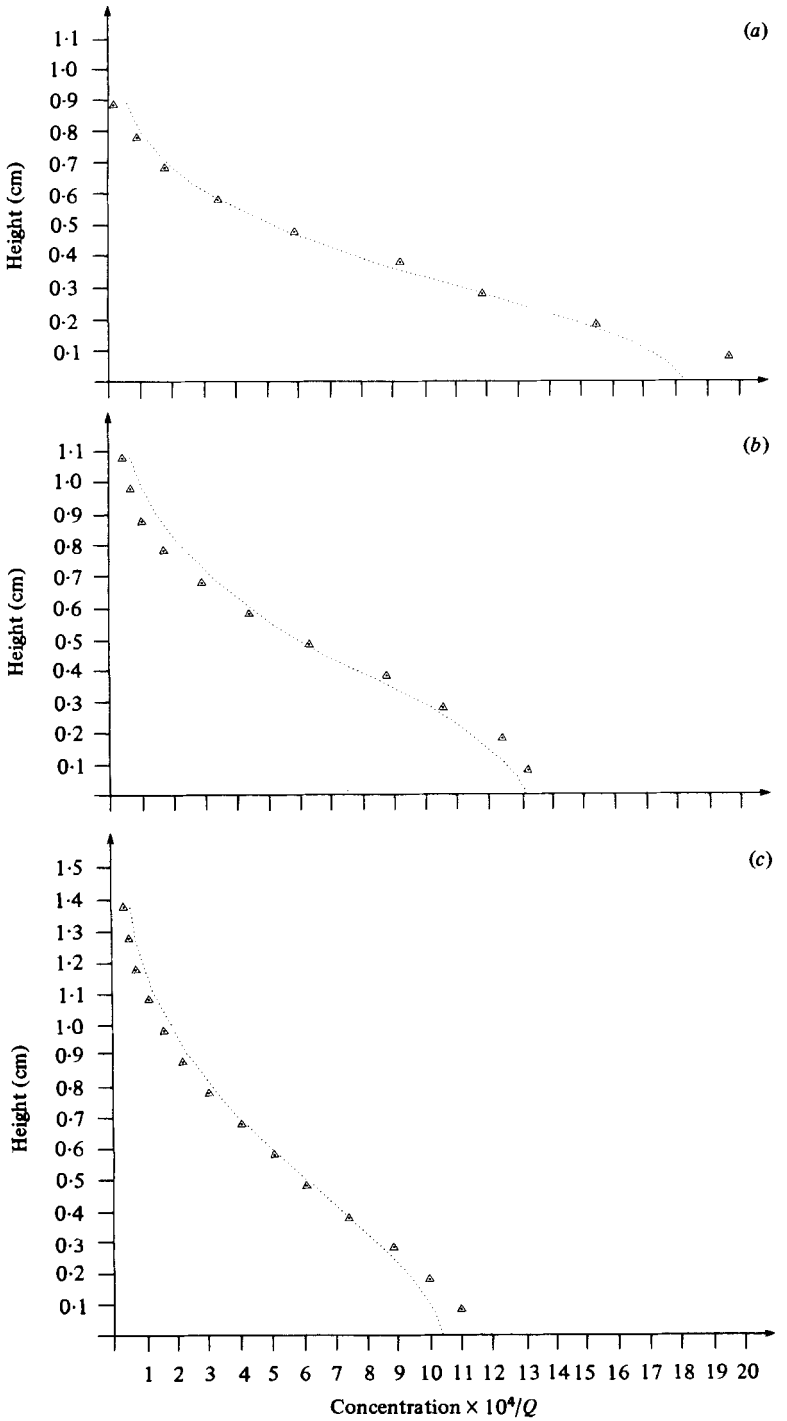

FIGURE 7. Vertical distribution of concentration at various downstream distances over a flat surface from a line source. $Q = 0{\cdot}0052$ g s^{-1} cm^{-1}, $u_0 = 2150$ cm/s. (*a*) 6 cm from line source; (*b*) 10 cm from line source; (*c*) 14 cm from line source. △ △ △ △, experiment; · · ·, calculated values (from Davies & Bourne's method).

ridge is then put in place, as in the momentum transfer experiments, and concentration readings are taken at downstream positions on the ridge, using mainstream velocities of 1540 cm s^{-1}, 1870 cm s^{-1} and 2150 cm s^{-1}. The results measured at the flow speed of 2150 cm s^{-1} are shown in figure 8; these were obtained over the leading and back slopes of the ridge: the sampling positions shown in figure 2 are used and the line source is placed 1·6 cm upstream of the commencement of the ridge.

5. Conclusions

An open-circuit wind tunnel was used to measure the distribution of mean velocity profile over the mid-section of a ridge of small slope, placed on the floor of the working section of the tunnel, three tunnel speeds being used. These were compared with theoretical calculations, based on the following premises.

(i) The pressure gradient generated by the ridge near its surface can be deduced from classical inviscid flow over a circular cylinder, radius a; this is consistent with the rigorous analysis developed by Sykes (1980).

(ii) Terms of higher order than $(aU_0/\psi)^2$ (a parameter which measures the curvature of the ridge surface for a given flow system) can be neglected.

(iii) Second-order terms of velocity perturbation can be neglected in the equations of mean motion.

Apart from a region close to the surface on the down-slope side of the ridge, agreement between theory and experiment was seen to be extremely good.

Measurements were also made of rates of evaporation from varying lengths of Whatman No. 1 filter paper placed on the up-slope side of the ridge, the gravimetric method being employed. These showed a 20–25 % increase of evaporation rate from the lowest to the highest part of the ridge. A previous theoretical formulation by Davies & Bourne (1956) was modified to apply to the curved surface studied, and was seen to be in good agreement with experiment. This can be extended to predict mass transfer from curved surfaces of small slopes, for any prescribed spatial distribution of surface concentration of the quantity being transferred: it can also be applied to calculate heat transfer from similar curved surfaces for prescribed surface temperature distributions.

This method of analysis is also used to predict concentration profiles downstream of a line source placed in a turbulent boundary layer over a flat plate in a wind tunnel. It is found that theory and experiment match each other extremely well, as borne out by figure 7. The eddy-viscosity form used by Davies & Bourne (1956) in their flat-plate analysis is then adapted to approximate to the eddy-viscosity distribution over the limited range of downstream distance covered by the leading slope of the ridge, the velocity form used being identical with that used in the mass transfer case. The resulting solution works well over most of the leading slope of the ridge. The important point to note in figure 8 is that it predicts accurately the decrease in concentration caused by additional turbulent momentum drawn in from above the surface and the downstream 'stretching' by higher velocities over the ridge. These results illustrate the significant effect of surface curvature on diffusion. It is suggested that these processes enhance the diffusing properties, and hence the concentration is decreased as the wind speed increases. On the back slope of the ridge the flow is retarded close to the surface, leading to an increase in the concentration in this region: however, further away from

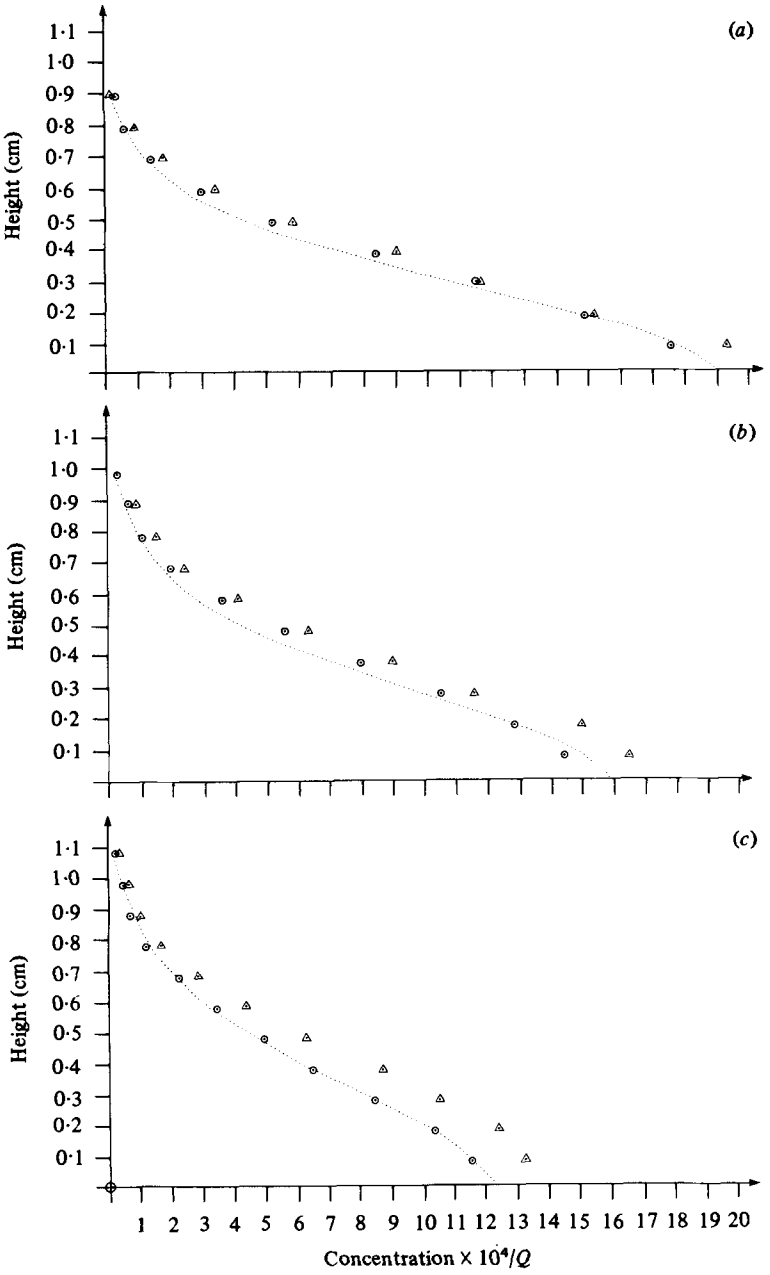

FIGURE 8. For legend see facing page.

the surface the flow returns to its previous increase in velocity and the concentration decreases again compared to that in flat-plate flow.

The assumption that the parameter q used in the velocity profiles is constant over a limited range of downstream distance gives rise to reasonable approximations to these profiles over the leading slope of the ridge. However, over the brow of the ridge the approximation has its largest discrepancy; theory and experiment do not agree as

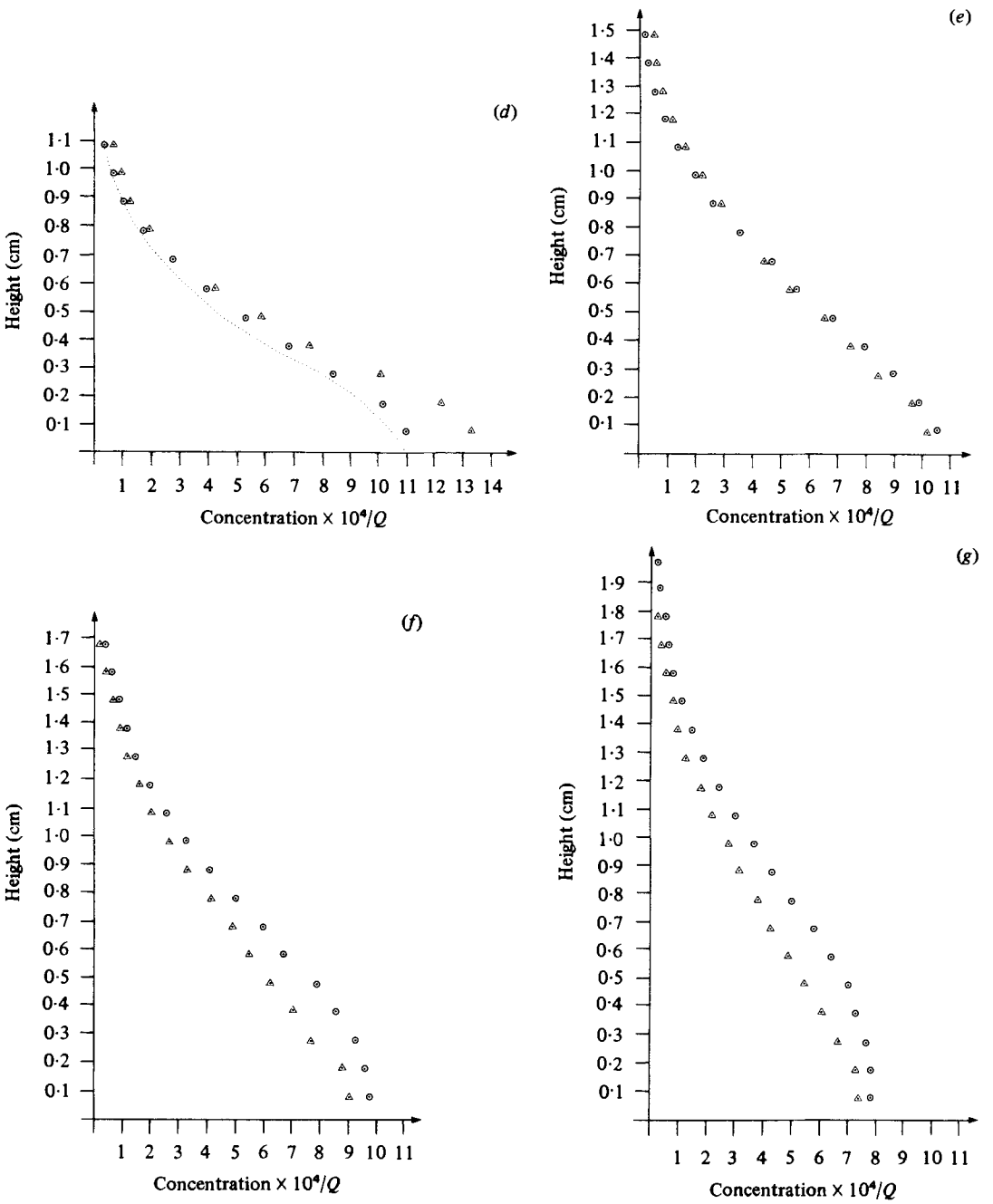

FIGURE 8. Vertical distribution of concentration at various downstream distances over a ridge and flat surface from a line source. $Q = 0{\cdot}0052$ g s^{-1} cm^{-1}; $u_0 = 2150$ cm/s; (*a*) 6 cm from source, (*b*) 7·6 cm from source (position 3), (*c*) 10 cm from source, (*d*) 11·6 cm from source (position 4), (*e*) 15·6 cm from source (position 5), (*f*) 19·6 cm from source (position 6), (*g*) 23·6 cm from source (position 7). △△△△, experiment (flat surface); ⊙⊙⊙⊙, experiment (ridge surface); ···, calculated from ridge theory.

well as at lower positions. The choice of eddy-viscosity distribution proved to be very important; other possible forms of approximation were tried, based on, for example, mixing-length; but they did not lead to results that agreed very well with experiment. However, the eddy-viscosity form derived from Davies & Bourne's flat-plate method of calculation, and applied in the region away from the surface, leads to good agreement between theory and measurement.

These results indicate the sharp effect on mean velocity distribution (and associated surface mass transfer) of curvature due to the additional velocities generated by the induced pressure gradients. This effect could well be of considerable importance in engineering, meteorological and agricultural contexts.

The theoretical analysis is capable of extension to axially symmetric boundary surfaces, such as flow along a long circular cylinder or radially out along a rotating disk, followed by flow over radially symmetrical small-sloped protuberances on these surfaces. By using suitable forms of mapping in the initial pressure gradient calculation, it can also be applied to other forms of topography.

The authors are deeply indebted to various members of staff and technicians of the Exeter University Applied Science Departments for technical help and encouragement; in particular Dr M. A. Patrick, Dr H. Zienkiewicz, Mr M. Jenkins and Mr D. Walsh. R. A. Dawkins gratefully acknowledges the financial aid of a N.E.R.C. (U.K.) Research Studentship. We are also grateful for the helpful comments supplied by Dr R. I. Sykes (formerly at the Meteorological Office).

REFERENCES

DAVIES, D. R. & BOURNE, D. 1956 On the calculation of heat and mass transfer in laminar and turbulent boundary layers. *Quart. J. Mech. Appl. Math.* **9**, 457.

DAVIES, D. R. & WALTERS, T. S. 1952 Further experiments on evaporation from small, saturated, plane areas into a turbulent boundary layer. *Proc. Phys. Soc.* B **65**, p. 640.

DAWKINS, R. A. 1979 Ph.D. thesis, Exeter University.

HOWARTH, L. 1953 *Modern Developments in Fluid Dynamics.* Oxford University Press.

HUNT, J. C. R. & MULHEARN, P. J. 1973 Turbulent dispersion from sources near two-dimensional obstacles. *J. Fluid Mech.* **61**, 245.

JACKSON, P. S. & HUNT, J. C. R. 1975 Turbulent wind flow over a low hill. *Quart. J. Roy. Met. Soc.* **101**, 922.

PASQUILL, F. 1943 Evaporation from a plane free-liquid surface into a turbulent air stream. *Proc. Roy. Soc.* A **182**, 75.

SUTTON, O. G. 1953 *Micrometeorology.* McGraw-Hill.

SYKES, R. I. 1980 An asymptotic theory of incompressible turbulent boundary layer over a small hump. *J. Fluid Mech.* **101**, 647.

TAYLOR, P. A. 1977 Numerical studies of neutrally stratified planetary boundary layer flow over gentle topography. *Boundary-Layer Met.* **12**, 37.